

# COMPARISON OF THE KSC-ER CLOUD-TO-GROUND LIGHTNING SURVEILLANCE SYSTEM (CGLSS) AND THE U.S. NATIONAL LIGHTNING DETECTION NETWORK™ (NLDN)

\*Jennifer G. Ward,<sup>1,2</sup> Kenneth L. Cummins<sup>1,3</sup> and E. Philip Krider<sup>1</sup>

<sup>1</sup>Institute of Atmospheric Physics, University of Arizona, Tucson, Arizona

<sup>2</sup>Also National Aeronautics and Space Administration/Kennedy Space Center, Florida

<sup>3</sup>Also Thunderstorm Business Unit, Vaisala, Inc., Tucson, Arizona

## Introduction

The NASA Kennedy Space Center (KSC) and Air Force Eastern Range (ER) are located in a region of Florida that experiences the highest area density of lightning strikes to ground in the United States, with values approaching 16 fl/km<sup>2</sup>/yr when accumulated in 10x10 km (100 km<sup>2</sup>) grids (see Figure 1). Consequently, the KSC-ER use data derived from two cloud-to-ground (CG) lightning detection networks to detect hazardous weather, the "Cloud-to-Ground Lightning Surveillance System" (CGLSS) that is owned and operated by the Air Force and the U.S. National Lightning Detection Network (NLDN™) that is owned and operated by Vaisala, Inc. These systems are used to provide lightning warnings for ground operations and to insure mission safety during space launches at the KSC-ER. In order to protect the rocket and shuttle fleets, NASA and the Air Force follow a set of lightning safety guidelines that are called the Lightning Launch Commit Criteria (LLCC). These rules are designed to insure that vehicles are not exposed to the hazards of natural or triggered lightning that would in any way jeopardize a mission or cause harm to the shuttle astronauts. Also, if any CG lightning strikes too close to a vehicle on a launch pad, it can cause time-consuming mission delays due to the extensive retests that are often required for vehicles and/or payloads when this occurs. If any CG lightning strike is missed or mis-located by even a small amount, the result could have significant safety implications, require expensive retests, or create unnecessary delays or scrubs in launches. Therefore, it is important to understand the performance of each lightning detection system in considerable detail.

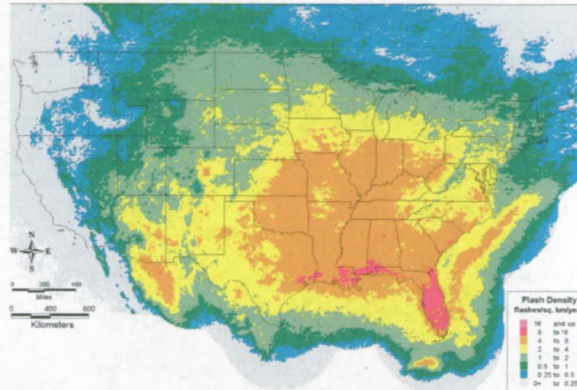


Figure 1. Map of the annual area density of CG lightning in the U.S. for years 1996 – 2005 (Courtesy Vaisala, Inc.).

Given the mission-critical nature of the NLDN and the CGLSS, a comparison of the detection efficiency and location accuracy of these lightning detection systems was carried out in 1996 (Maier and Wilson, 1996) after an upgrade to the NLDN in 1995 (Cummins et al., 1998). At that time, the NLDN was found to have a flash detection efficiency of 90% and a median location accuracy of 0.6 km, based on comparisons with CGLSS. Since 1996, both networks have undergone additional upgrades to improve performance, and this warrants a re-examination of the relative performance of both networks. The 1998 CGLSS upgrade added a sixth sensor and implemented a location algorithm that included time-of-arrival information. These upgrades increased the flash detection efficiency of CGLSS inside the network to ~98% and the location accuracy to ~250m from the previous 92% and 500m, respectively (Boyd, et al, 2000). The 2002-2003 upgrades to the NLDN included replacing all of the old sensors, a combination of out-dated time-of-arrival LPATS and early IMPACT sensors, with a uniform network of IMPACT ESP sensors (Cummins et al, 2006). This increased the overall sensitivity and accuracy of the NLDN,

\*Corresponding author address:

Jennifer G. Ward, NASA KSC, KT-C-H,  
Kennedy Space Center, FL 32899;  
E-mail: Jennifer.G.Ward@nasa.gov

particularly near the boundaries of the network (Biagi et al., 2007).

Here, we will examine specific subsets of CG strokes and flashes that were reported individually and in-common by the NLDN and CGLSS networks. We will evaluate the fraction of CGLSS “strike points” that are reported by the NLDN (relative NLDN strike-point DE), the spatial separation between the strike points that are reported by both networks (relative location accuracy), and the values of the estimated peak current,  $I_p$ , that are reported by both networks. Where possible, these results will also be compared to the findings of Maier and Wilson (1996), which were obtained prior to the most-recent upgrades of both networks.

### NLDN and CGLSS Instrumentation

The NLDN is a national network of 113 IMPACT ESP sensors<sup>4</sup> that are placed 200-350 km apart. Figure 2 shows the evaluation region (100 km radius) at the KSC-ER and its location relative to the 10 closest NLDN sensors (black triangles). The three closest NLDN sensors to the KSC-ER are in Palm Bay, Tampa, and Ocala, FL. The NLDN processes data in the following sequence: sensors detect an electromagnetic pulse that is characteristic of a return stroke in CG lightning; the GPS time, amplitude, polarity, and direction of the stroke are transmitted via satellite communications to a network control center in Tucson, Arizona; information derived from multiple sensors is used to geo-locate the event and estimate the peak current (and polarity) of each stroke; and finally lightning information is forwarded to users in real-time via either terrestrial or satellite data links. This entire process takes approximately 30-40 seconds (Cummins et al., 2006).

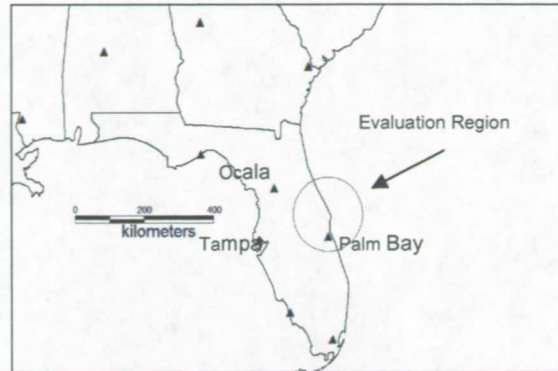


Figure 2. Evaluation region centered at the KSC-ER and the locations of the nearest NLDN sensors.

The CGLSS is a local network that covers the KSC-ER operations area with 6 medium gain IMPACT ESP sensors located ~30km apart. The CGLSS data processing steps are similar to the NLDN, except that land-line communications are used instead of satellite links and the control center is located at the ER. The sensor locations are shown in Figure 3 (black triangles).

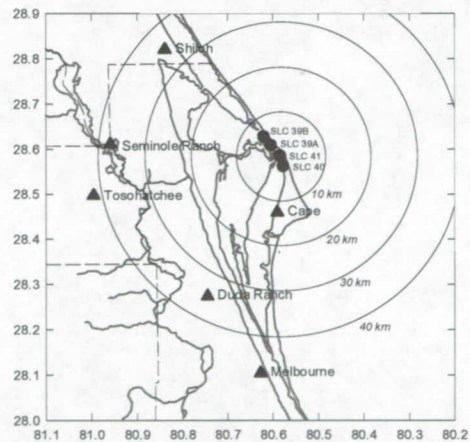


Figure 3. Location of the CGLSS sensors near the KSC-ER.

The NLDN and CGLSS systems differ somewhat in their processing of the lightning information. Currently, the NLDN locates all detected strokes, optionally groups them into flashes, and then estimates the peak current ( $I_p$ ) of each stroke by scaling the range-normalized signal strength by a factor of 0.185 (Cummins et al., 2006). The reported time is the estimated time-of-occurrence of the stroke at the stroke location.

<sup>4</sup> Manufactured by Vaisala Inc., Tucson, AZ

The CGLSS on the other hand, locates the first stroke in each flash and those subsequent strokes that have strike locations that are more than 0.5 km from the first-stroke location (Maier and Wilson, 1996). In the following, we will refer to both of these types of events as "CGLSS strokes." The CGLSS estimates  $I_p$  by scaling the range-normalized signal strength by a factor of 0.23. The CGLSS event time is the time that the radiated lightning waveform exceeds a fixed detection threshold at the nearest reporting sensor. Therefore, the CGLSS times can be up to  $\sim 200 \mu\text{s}$  after the time-of-occurrence of the NLDN strokes in the evaluation region. When the CGLSS detects more than one stroke at the same location, it reports the highest  $I_p$  of any stroke in the flash at that location.

## Methods

### Case Selection Process

Counts of CGLSS lightning strokes during the summers of 2005 and 2006 (June through August) were examined, and then the four days that had the most counts with events in all directions around the KSC-ER were chosen for further analysis (June 15, 17, and August 1, 2005 and July 23, 2006). Next, all CGLSS "flashes" (new strike points) within 100 km of an origin near the Space Shuttle launch complex were compared with the NLDN stroke reports in the same region. Figure 4 shows the locations of all lightning events on July 23, 2006. The locations of all NLDN strokes (14,457) are shown as blue diamonds, the CGLSS stroke reports (3,565) as magenta squares, and the central origin is a red dot. (Here, the number of NLDN strokes is much larger than the number of CGLSS strokes because the CGLSS excludes subsequent strokes in the same channel.)

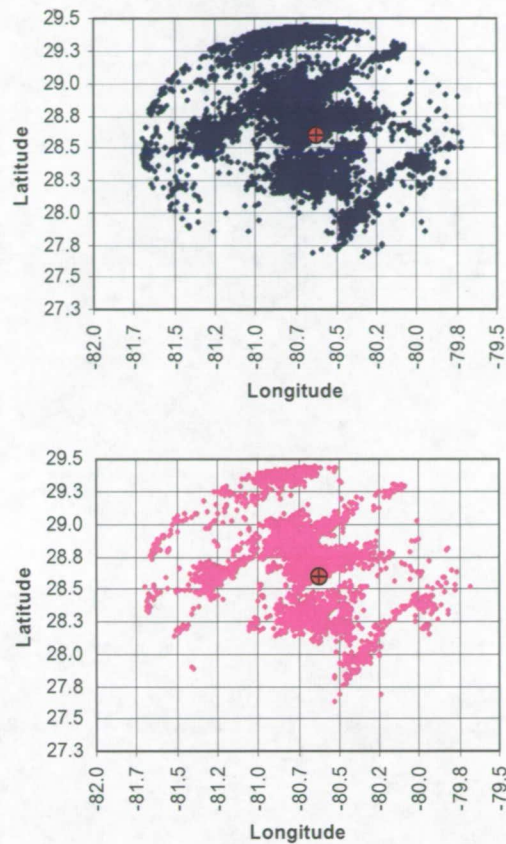


Figure 4. The locations of CG lightning strokes reported by NLDN (top) and CGLSS (bottom) on July 23, 2006.

### Data and Data Processing

The NLDN data were obtained from a Vaisala data archive that contains, for each stroke, the GPS date and time (to the ms), latitude and longitude (in degrees),  $I_p$  (in kA), the length of the semi-major axis of the 50% confidence ellipse, (in km) and its orientation, the chi-square value for the computed location, and the number of sensors reporting the stroke (NSR). A sample of these data is shown in Table 1.

Table 1. A portion of the NLDN data provided by Vaisala Inc. The units of the semi-major axis are km.

Date	HH:MM:SS.ms	Latitude	Longitude	$I_p$ (kA)	semi-major	chi-squ.	NSR
6/15/2005	16:49:30.042	29	-81.166	-23.3	0.4	0.4	10
6/15/2005	16:59:50.218	28.982	-81.16	3.4	4.5	0.7	2
6/15/2005	17:02:33.828	28.953	-81.197	-7.6	1	0.6	3
6/15/2005	17:02:33.931	28.957	-81.194	-8.5	0.9	0.8	4
6/15/2005	17:05:17.896	28.956	-81.18	21.9	0.5	0.9	8
6/15/2005	17:05:17.925	28.943	-81.178	-20.1	0.4	0.7	9
6/15/2005	17:05:17.974	28.963	-81.182	-17.5	0.4	0.4	8
6/15/2005	17:05:18.035	28.963	-81.173	-10.2	1.1	0.2	3
6/15/2005	17:06:42.339	28.944	-81.171	-27.7	0.4	0.4	11
6/15/2005	17:06:42.435	28.944	-81.172	-13.5	0.5	0.4	6
6/15/2005	17:06:42.491	28.948	-81.17	-4.2	1.1	1.1	3
6/15/2005	17:06:42.595	29.002	-81.162	-5.7	6.2	0.2	2
6/15/2005	17:06:42.668	28.945	-81.175	-6.2	1.1	1.1	3
6/15/2005	17:13:42.547	28.944	-81.154	11.8	0.5	0.5	6
6/15/2005	17:19:00.549	29.042	-80.929	-19.2	0.5	0.5	6
6/15/2005	17:21:57.551	29.058	-80.935	-27.1	0.4	0.6	11
6/15/2005	17:21:57.553	29.025	-81.004	-6.1	9.7	0.8	2
6/15/2005	17:21:57.586	29.041	-80.938	-9.4	1.2	0.5	4

The CGLSS data were provided by Computer Sciences Raytheon, Patrick Air Force Base, FL, and delivered in a standard APA output format. They were then reformatted to match, as closely as possible, the same fields as the NLDN data. A sample of the reformatted CGLSS data is given in Table 2.

Table 2. Reformatted CGLSS data. The units of the semi-major and semi-minor axes are nm.

HH:MM:SS.ms	Date	Latitude	Longitude	Mult	$I_p$ (kA)	chi squ.	semi-major	semi-minor
16:49:30.042	6/15/05	29	-81.166	1	-25.1	0.7	0.4	0.1
17:02:33.828	6/15/05	28.945	-81.176	2	-8.7	1.1	0.4	0.1
17:05:17.925	6/15/05	28.941	-81.177	3	-22	0.5	0.3	0.1
17:06:42.339	6/15/05	28.941	-81.169	5	-29.3	0.5	0.3	0.1
17:19:00.550	6/15/05	29.045	-80.928	1	-25.5	1.2	0.6	0.1
17:21:57.552	6/15/05	29.071	-80.935	2	-30.3	0.8	0.6	0.1
17:23:53.021	6/15/05	29.077	-80.813	1	-17.4	1.2	0.8	0.1
17:26:32.804	6/15/05	29.045	-80.904	1	-43.7	0.9	0.5	0.1
17:33:13.324	6/15/05	28.917	-80.859	1	-21.7	1	0.4	0.1
17:33:54.160	6/15/05	28.919	-80.82	1	-18.5	4.2	0.6	0.1
17:34:09.571	6/15/05	28.873	-80.844	1	-13.3	6.6	0.3	0
17:34:37.743	6/15/05	28.898	-80.847	1	-16.8	0.9	0.4	0.1
17:35:36.866	6/15/05	28.904	-80.841	2	-25.4	1.6	0.3	0
17:36:20.597	6/15/05	28.885	-80.827	1	-10.8	5.7	0.7	0
17:39:16.852	6/15/05	28.921	-80.854	1	-25.6	0.5	0.4	0.1

The NLDN and CGLSS strokes were considered to be time-correlated if the CGLSS event time was within a 2 ms interval after the time of the corresponding NLDN event. Only time-correlated events were used in the comparison of  $I_p$  values (linear regression), analysis of the relative detection efficiency, and the analysis of location accuracy. The detection efficiency analysis was carried out for negative first strokes and negative subsequent strokes that produced new ground contacts (as reported by the CGLSS). The percentages of CGLSS events that were reported by the NLDN were computed

as a function of  $I_p$ , and the percentages of NLDN events that were reported by the CGLSS were computed when  $|I_p| \geq 50$  kA. The location accuracy analysis consisted of computing the horizontal distances between the time-correlated stroke locations (both positive and negative polarity) in kilometers.

## Results and Discussion

### Peak Current Analysis

Figure 5 shows a scattergram of the relationship between the NLDN  $I_p$  values (x-axis) and the CGLSS  $I_p$  values (y-axis) for all time-correlated strokes on July, 23 2006. This day is representative of the entire dataset. This figure also shows that the regression coefficient is 1.1066 with an  $R^2$  value of 0.8986 which means that 90% of the variance can be explained by a linear relationship between these variables. Note that the  $I_p$  values are highly correlated over a range of  $\pm 150$  kA, and that the largest scatter is for high-current positive and low-current negative strokes. The RMS error (average standard deviation in y) was 2.8 kA. On average, the CGLSS estimates of  $I_p$  are slightly higher than the NLDN. This difference was expected because of the different scaling values (0.23 for CGLSS and 0.185 for NLDN) that are used for the field-to-current relationship discussed above. This scaling difference predicts a slope of 1.23 (0.23/0.185), which is within 10% of the empirically-derived slope (1.107). The remaining difference is likely associated with differences in the propagation models that are used to compute the range-normalized signal strengths, since the fields produced by flashes in the evaluation region must propagate 3 to 6 times farther to the NLDN sensors than to the CGLSS sensors.

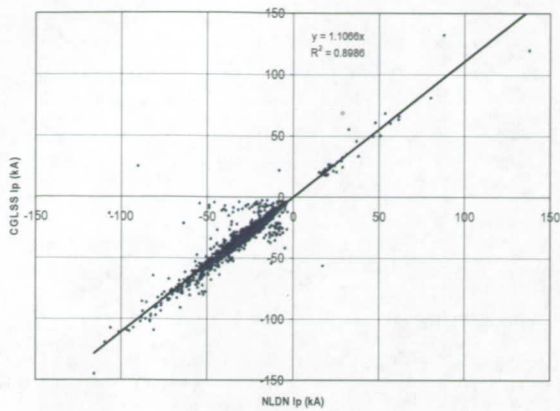


Figure 5. CGLSS  $I_p$  values vs. the corresponding NLDN  $I_p$  values.

### Detection Efficiency

The NLDN detection efficiency (DE) relative to the CGLSS on July, 23 2006, is shown in Figure 6. The blue diamonds in Figure 6a show the fraction of NLDN strokes reports relative to the CGLSS reports, with the value "1.00" meaning 100% detected. Each diamond shows the average value over that 2 kA bin. The error bars show values of  $\sigma$  computed for a normalized binomial distribution using the relation

$$\sigma = \sqrt{p(1-p)/n}$$

Here,  $\sigma$  is the standard deviation of the distribution,  $p$  is the fraction of strokes detected by the NLDN, and  $n$  is the total number of strokes in each bin. The bar graph in Figure 6b shows the total number of CGLSS events (red) that are in each 2 kA bin of  $I_p$  as well as the total number of time-correlated (TC) NLDN events (blue) in that bin. The NLDN reported less than half of the strokes that had an estimated  $|I_p|$  between 2 and 4 kA, but the DE steadily increased to 90% or more above 10 kA. The NLDN failed to detect 17.5 % of the CGLSS-reported negative strokes that had  $|I_p| < 12$  kA. Since 12% of the negative CGLSS strokes on this day were less than 12 kA, the total percentage of strike points missed by the NLDN was approximately 2%. These percentages also hold true for the entire dataset. Failure of the NLDN to report low-current strokes was

expected, because of the much larger sensor baseline distances in the NLDN.

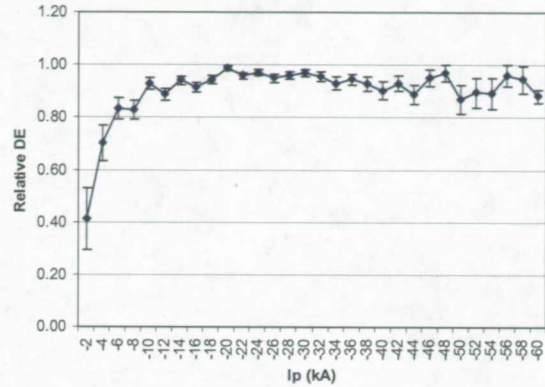


Figure 6a. Fraction of NLDN strokes relative to CGLSS strokes as a function of  $I_p$ .

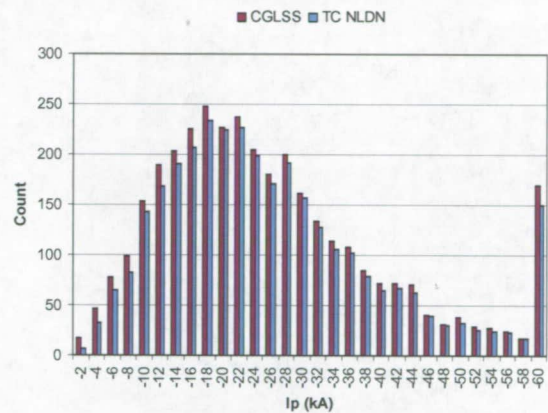


Figure 6b. Number of CGLSS strokes (red) and time-correlated NLDN strokes (blue) as a function of  $I_p$  ( $2 \text{ kA} < |I_p| < 150 \text{ kA}$ ).

Given the short sensor baselines and the low number of sensors in the CGLSS, one can readily imagine cases where high-current strokes could saturate most (or all) of the CGLSS sensors and produce inconsistent measurements among the sensors. The NLDN is less likely to miss high-current strokes because of its longer baselines and the larger number of sensors in that network. In order to explore this possibility further, we have compared the reports of high-current negative strokes, i.e. strokes with  $|I_p| \geq 50$  kA, in the evaluation region. The CGLSS  $I_p$  values were corrected to match the NLDN  $I_p$  values using the regression slope in Figure 5; then strokes

reported by two or more CGLSS sensors (including those not reported as first strokes or new ground strike points) were compared to the high-current NLDN reports that were time-correlated with CGLSS.

Histograms of the NLDN and CGLSS counts vs. the NLDN  $I_p$  values on July 23, 2006 are shown in Figure 7. The blue bars show the total number of strokes reported by the NLDN and the red bars show the number of time-correlated CGLSS strokes. The 0.1 bin shows counts of the time-correlated negative events that NLDN reported with  $|I_p| \geq 50$  kA but the CGLSS reported with  $|I_p| < 50$  kA. Based on the measurements for all days, the CGLSS failed to report about 28% of the high-current strokes that were reported by the NLDN. Since only about 10% of the negative strokes have an  $|I_p| \geq 50$  kA, the total percentage of the large events that was missed by the CGLSS (due to a high  $I_p$ ) is approximately 2.8%.

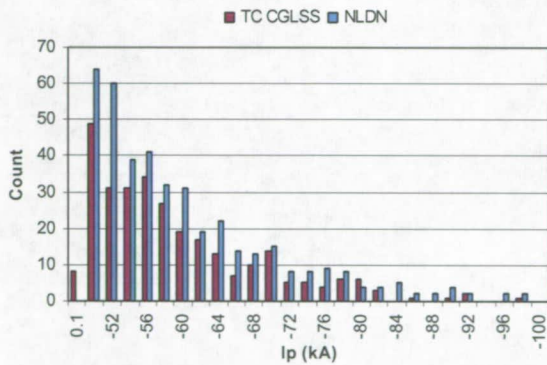


Figure 7. Number of negative NLDN strokes (blue) and time-correlated CGLSS strokes (red) as a function of  $I_p$  (for  $|I_p| \geq 50$  kA) on July 23, 2006.

### Location Accuracy

Analysis of the relative location accuracy of the two networks on July 23, 2006 is shown in Figure 8. Here, distance (location difference) bins of 200 m are plotted on the x-axis, and the primary y-axis shows the number of time-correlated events that were in each bin. The secondary y-axis is a cumulative distribution that

shows the total fraction of time-correlated events with a location difference that is less than or equal to that distance (blue diamonds). The median position difference (50<sup>th</sup> percentile) is 683 m on this day and 656 m overall on the four days that were analyzed.

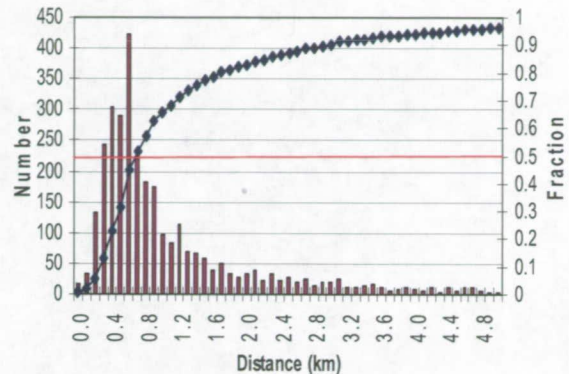


Figure 8. Distributions of the horizontal distances between time-correlated, negative CGLSS and NLDN locations.

### Discussion and Conclusions

First, it is clear that the upgrades to the NLDN and CGLSS have improved their overall performance. The  $I_p$  values from each network are highly correlated over a range of  $\pm 150$  kA, and the largest scatter is for high-current positive and low-current negative  $I_p$  values. Once the different scaling factors (0.23 for CGLSS and 0.185 for NLDN) were accounted for, a regression slope near unity was achieved.

Both systems appeared to detect most of the strokes that produced new ground strike points, with some specific exceptions. The NLDN failed to report 313 out of 1789 (17.5%) of the CGLSS negative first strokes (and subsequent strokes that produce new ground contacts) that had  $|I_p| < 12$  kA. However, the NLDN detection threshold was improved (lowered) by the upgrade in 2002-2003. This is reflected by the fact that CGLSS-reported strokes with  $|I_p|$  above 12 kA were reported more than 95% of the time by the upgraded NLDN, whereas this level of detection was not present in 1996. Formerly, the best DE

(90%) occurred for strokes with  $|I_p|$  above 15 to 20 kA (Maier and Wilson, 1996 – Figure 4). The CGLSS failed to report 444 out of 1591 (28%) of the NLDN high-current strokes. In summary, the NLDN failed to report about 2% of all events (primarily low- $I_p$  strokes) and the CGLSS failed to report about 2.8% of all events (primarily high- $I_p$  strokes).

The relative location accuracy between the two networks is consistent with Vaisala model estimates of a 300m median location error for CGLSS and a 600-700m median error for the NLDN in this geographic region (Cummins et al, 1998). Assuming that the NLDN and CGLSS errors are uncorrelated, the expected median difference would be about  $(300^2 + 600^2)^{1/2}$  or ~670m, and this is consistent with our measured median of 656m. We note that the median position difference found in 1996 was 800m. Given that a much larger fraction of low-current events are now located by both networks, and the fact that low-current strokes do have inherently larger location errors, this result can be viewed as a modest but clear improvement in both networks.

Failure of the CGLSS to report about 28% of the high-current NLDN strokes and the NLDN to report about 17.5% of the low current CGLSS strokes clearly highlights the importance of using both networks to meet all the operational requirements at the KSC-ER.

### Acknowledgement

This work has been supported in part by the NASA Kennedy Space Center, Grant NNK06EB55G, the Vaisala Inc. Thunderstorm Business Unit, Tucson, AZ, and Computer Sciences Raytheon, Patrick Air Force Base, FL.

### References

Biagi, C.J., K.L. Cummins, K.E. Kehoe, and E.P. Krider, 2007: National Lightning Detection Network (NLDN) performance in southern Arizona, Texas, and Oklahoma in 2003-2004. *J. Geophys. Res.*, 112, D05208, doi:10.1029/2006JD007341.

Boyd, B.F., W.P. Roeder, D.L. Hajek, and M.B. Wilson, 2005: Installation, Upgrade, and Evaluation of a Short Baseline Cloud-to-Ground Lightning Surveillance System used to Support Space Launch Operations, AMS Conference on Meteorological Applications of Lightning Data, San Diego, CA, 9 – 13 January.

Cummins, K. L., J. A. Cramer, C. J. Biagi, E. P. Krider, J. Jerauld, M. A. Uman, and V.A. Rakov, 2006: The U.S. National Lightning Detection Network: Post-upgrade status, 2nd AMS Conference on Meteorological Applications of Lightning Data, Atlanta, GA, 29 January – 2 February.

Cummins, K. L., M. J. Murphy, E. A. Bardo, W. L. Hiscox, R. B. Pyle, and A. E. Pifer, 1998: A combined TOA/MDF technology upgrade of the U.S. National Lightning Detection Network, *J. Geophys. Res.*, **98**, 9035-9044.

Maier, M. W. and M. B. Wilson, 1996: Accuracy of the NLDN Real-Time Data Service at Cape Canaveral, Florida, Int. Lightning Detection Conference, Tucson, AZ, 6 – 8 November.